An Adaptive Passive Radio Map Construction for Indoor WLAN Intrusion Detection

Yixin Lin(✉), Wei Nie, Mu Zhou, Yong Wang, and Zengshan Tian

Chongqing Key Lab of Mobile Communications Technology, Chongqing University of Posts and Telecommunications, Chongqing 400065, China
260150244@qq.com, linyixin_cqupt@foxmail.com,
{niewei,zhoumu,tianzs}@cqupt.edu.cn, dr_ywang@hotmail.com

Abstract. Indoor WLAN intrusion detection technique for the anonymous target has been widely applied in many fields such as the smart home management, security monitoring, counterterrorism, and disaster relief. However, the existing indoor WLAN intrusion detection systems usually require constructing a passive radio map involving a lot of manpower and time cost, which is a significant barrier of the deployment of WLAN intrusion detection systems. In this paper, we propose to use the adaptive-depth ray tree model to automatically construct an adaptive passive radio map for indoor WLAN intrusion detection. In concrete terms, the quasi-3D ray-tracing model is enhanced by using the genetic algorithm to predict the received signal strength (RSS) propagation feature under the indoor silence and intrusion scenarios, which improves the computational efficiency while preserving the accuracy of passive radio map. Then, the RSS mean, variance, maximum, minimum, range, and median are allied to increase the robustness of passive radio map. Finally, we conduct empirical evaluations on the real-world data to validate the high intrusion detection rate and low database construction cost of the proposed method.

Keywords: Indoor intrusion detection · Adaptive ray-tracing · Passive radio map · Genetic algorithm · WLAN

1 Introduction

With the wide deployment of wireless local area network (WLAN) and general support of WLAN protocol by various intelligent terminals, the intrusion detection with respect to the indoor target can be realized by using the existing WLAN infrastructure. Among the existing anonymous target intrusion detection techniques, the wireless local area network (WLAN) indoor target intrusion detection system [1–4] proposed by the University of Maryland performs outstandingly

Q. Liang et al. (eds.), *Communications, Signal Processing, and Systems*, Lecture Notes in Electrical Engineering 516,
https://doi.org/10.1007/978-981-13-6504-1_156

because it can effectively protect the user's location privacy and work stably under non-line-of-sight and without special hardware at the same time. However, the main problem with this kind of algorithms is that the construction of the prior passive radio map takes a lot of manpower and time, which is a major barrier of WLAN intrusion detection systems deployment. On this basis, the WLAN indoor target intrusion detection algorithm proposed in this paper uses the adaptive-depth ray tree-based quasi-3D ray-tracing model to construct the passive radio map automatically, which requires less labor overhead compared with the traditional RSS feature database construction method. In addition, six signal characteristics of the passive radio map are constructed, which results in the better pattern recognition ability and learning convergence. The rest of this paper is structured as follows. In Sect. 2, we describe the proposed indoor WLAN intrusion detection method in detail, and the related experimental results are shown in Sect. 3. Finally, we conclude this paper in Sect. 4.

2 System Description

The overall flow of the system is shown in Fig. 1. First, a number of WLAN access points (APs) and monitor points (MPs) are arranged in the target area. Second, the GA algorithm is used to optimize the limited number of depth of the ray tree adaptively and the RSS characteristics under the indoor silence, and intrusion scenarios are constructed according to the optimized ray-tracing model. Then, the obtained RSS characteristics are used for probabilistic neural network (PNN) training. Finally, the trained PNN is used to classify the new observation RSS data by multiple classifications, so as to realize the intrusion detection and area localization.

2.1 Signal Prediction

Considering the limitations of the existing 2D and 3D ray-tracing models [5,6] on the accuracy of the signal prediction and the complexity of the algorithm respectively, the quasi-3D ray-tracing model used in this paper first carries out the ray-tracing in the 2D projection plane, and then transforms it into the propagation path in the 3D space, and this process significantly improves the computational efficiency while guaranteeing the accuracy of prediction. In this case, as shown in Fig. 2, a quasi-3D ray-tracing model based on the adaptive-depth ray tree is proposed in this paper, considering two factors: the model accuracy and calculation efficiency.

The import of environmental information. Figure 3 gives a 3D modeling of a simple environment and the corresponding 2D projection results. The gray and black parts of the diagram represent the boundary face of environment and the indoor facilities, respectively. In addition, in order to ensure the integrity of the imported environmental information, the 3D vertex coordinates, height information and relative permittivity, conductivity and permeability of the corresponding material will be recorded.

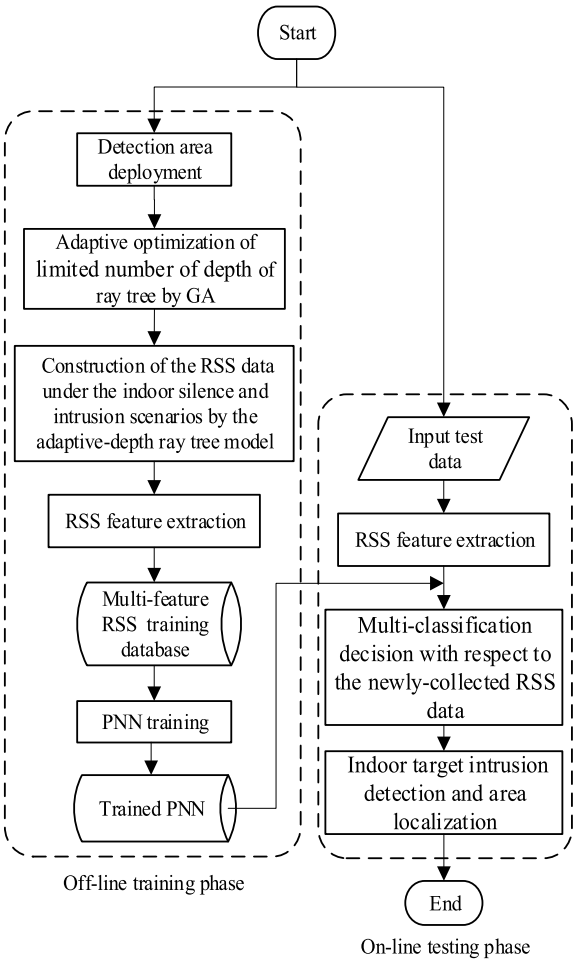

Fig. 1. Overall system flowchart

Optimization of the limited number of depth. In order to significantly improve the computing efficiency of the ray tree, the GA algorithm is used to optimize the limited number of depth of the ray tree in different environments. Specifically, first, the limited number of depth is initialized to 1; secondly, all the vertical planes and vertical lines of the 3D modeling of the environment are numbered; besides, the number of the functional parts of each ray is spliced into a chromosome in chronological order, and the field strength of each ray that reaches the MP is used as the fitness of its corresponding chromosome; then, the contribution rate of the ray to the field strength at MP under the condition of the current limited number of depth is calculated by Algorithm 1;

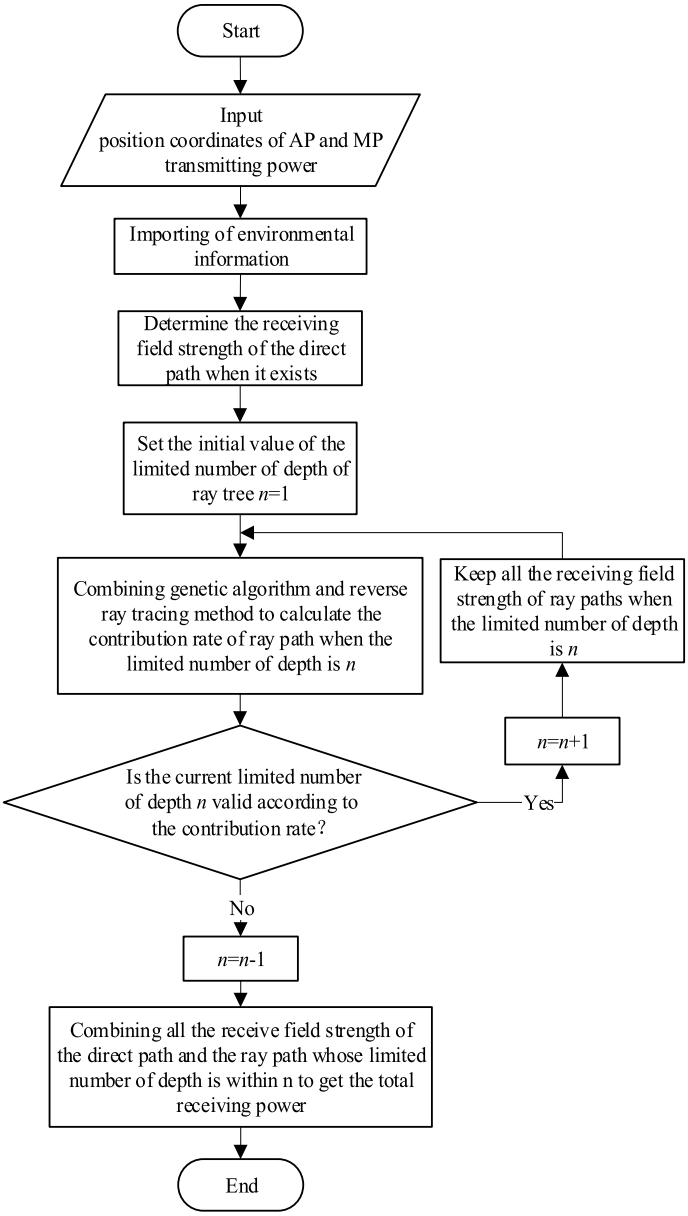

Fig. 2. Signal prediction flowchart

finally, determine whether the contribution rate of the ray under the current limited number of depth is greater than the preset threshold, and if so, add 1 to the limited number of depth and repeat the above steps, otherwise the current limited number of depth is the optimal limited number of depth (or the

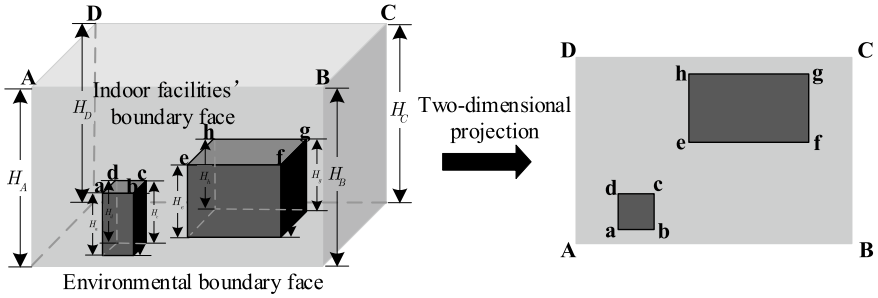

Fig. 3. 2D projection from 3D modeling of environment

Algorithm 1 Calculation of contribution rate of ray to the field strength

Input: n (the limited number of depth); $D_k(k{=}1, \ldots, N)$(the unique number of the kth functional part); N (the total number of the functional parts); P_{c} (crossover probability); P_{m} (mutation probability); M (population size); ρ_{th}(calculation rate threshold); e_{n-1}(maximum field strength of the n-1 order ray)

Output: C_n(contribution rate of the ray to the n order field strength)

The first generation population T_1 is randomly generated according to the limited number of depth n (that is, M random number sequences with a length of n), and set the current population $T = T_1$
while $\rho < \rho_{\mathrm{th}}$ **do**
    Use inverse ray-tracing method to calculate the fitness of each chromosome in current population T, namely e_1,...,e_M (as described in Algorithm 2)
    for i= 1:M **do**
        2 chromosomes were selected from T by fitness ratio selection algorithm[7]
        if random(0,1)< P_{c} **then**
            implement crossover operation on the selected 2 chromosomes
        end if
        if random(0,1)< P_{m} **then**
            implement mutation operation on the selected 2 chromosomes
        end if
        Add this 2 new chromosomes to the updated population T_{new}
    end for
    $T \Leftarrow T_{\mathrm{new}}$
    Compute $\rho = N_C/N^n$, and N_C is the number of chromosomes types that have appeared from the initial population to the current population
end while
Compute $T_f = e_{n-1}/2$
Compute m namely the number of chromosomes whose fitness> T_f in the current population T
Compute $C_n = m/M$

optimal ray order). In Algorithm 1, the fitness of each chromosome in the current population is calculated by the reverse ray-tracing method, and its calculation process is described in Algorithm 2.

Algorithm 2 Calculation of the n order chromosome fitness

Input: D_k(k=1, ..., N (the unique number of the kth functional part); N (the total number of the functional parts); P_k and H_k ($k = 1, \ldots, N_1$) (vertex coordinate and height information of the kth vertical lines); N_1 (the total number of the vertical lines); c_k ε_k and μ_k ($k = 1, \ldots, N_2$) (relative permittivity, conductivity and permeability of the kth vertical planes); N_2 (the total number of the vertical planes); λ (working wavelength); n (the limited number of depth); P_{AP} and P_{MP} (position coordinates of AP and MP); P_{t} (transmitting power of AP)

Output: e_i(chromosome fitness of the ith n order ray)

Assign B_k ($k = 1, \ldots, n+2$) according to the number sequence of functional part of the ith ($i = 1, \ldots, M$) n order ray, in which $B_1 = 1$ and $B_{n+2} = 1$ is the initial position of the ray AP and the termination position MP respectively; B_k=0 and 1 ($k = 2, \ldots, n+1$)represents reflection and diffraction occurs in the kth functional part respectively.
The 2D projection coordinates of AP and MP are L_1 and L_{n+2}, respectively
for $k = 2$: $n + 1$ **do**
    if $B_k = 0$ **then**
        $L_k \Leftarrow$ 2D projection coordinates of the mirror points of L_{k-1} with respect to the kth vertical planes
    else if $B_k = 1$ **then**
        $L_k \Leftarrow$ 2D projection coordinates of the kth vertical planes
    end if
end for
while there exists $k \in (1, ..., n)$ which makes $B_k = 1$ **do**
    if $B_k = 0$ and $B_{k+1} = 1$ **then**
        $L_k \Leftarrow$ 2D projection coordinates of the intersection point of the line connecting L_k and L_{k+1} and the kth vertical planes
        $B_k \Leftarrow 1$;
    end if
end while
for $k = 1 : n + 1$ **do**
    Set $T_{k,k+1}$ as the line connecting L_k and L_{k+1}
    if there exists the intersection of $T_{k,k+1}$ and any functional part **then**
        $e_i \Leftarrow 0$
        break;
    end if
end for
if $e_i \neq 0$ **then**
    The 2D projection of the ith n order ray extends to 3D space according to the Fermat principle, and then the fitness of the corresponding chromosome e_i is calculated
end if

Calculation of received signal power. In order to calculate the received signal power of MP, direct and non-direct rays are considered respectively. All the direct and non-direct rays within the n order are superimposed on the signal field strength, and the received signal power at MP can be obtained by the ray

power summation method [8] as

$$P_{total} = \sum_{i=1}^{l} \left(\frac{\lambda \left| \boldsymbol{E}_i \right|}{4\pi \left| \boldsymbol{E}_0 \right|} \right)^2, \tag{1}$$

in which $\boldsymbol{E}_0$ is the arrival signal field strength at 1 m from AP, and $\boldsymbol{E}_i$ is the arrival signal field strength of the ith ray, l is the total number of rays.

2.2 Intrusion Detection

In this paper, the kernel density estimation method based on Bayesian decision theory is applied to train the PNN feature data under the indoor silence and intrusion scenarios.[1] In particular, the kernel density function is used to estimate the conditional probability of different states, and then the state of the maximum posterior probability is used as the PNN output [9] according to the Bias decision theory. In order to ensure the stability of RSS characteristic data between each pair of AP and MP, this paper uses a sliding window function to segment the original RSS data[2] and calculates the mean, variance, maximum, minimum, maximum, and middle value of each segment data. On the basis of these six signal characteristics, six PNN structures are trained respectively. Finally, according to the voting criterion, the indoor target detection and location are realized by the multiclassification decision of the newly acquired RSS data.

3 Experimental Result

3.1 Environmental Layout

Figure 4 shows an experimental environment, in which two APs (AP1 and AP2 with model D-Link DAP 2310) and three MPs (MP1, MP2, and MP3 with model SAMSUNG GT-S7568) are placed at 2 and 0.5 m high, respectively. At each MP, 5 min of RSS data from each AP are collected separately under the indoor silence and intrusion scenarios.

3.2 GA Optimization Result

Figure 5 shows the change of the overall fitness of each generation of population under the conditions of different values of ρ_{th} when the GA was used to calculate the ray contribution rate. The overall fitness is defined as the ratio of m to the population size M, and m is the number of chromosomes whose fitness is greater than the threshold value T_f in the population. It can be seen that with the increasing of population algebra, the overall fitness is on the rise and tends to be the same when the population algebra reaches 30. In addition, Table 1

[1] Considering the content of water in the human body more than 70%, the human body is modeled as a 3D water column [10] with a certain height.

[2] The length of each segment of the RSS data is the width of the sliding window.

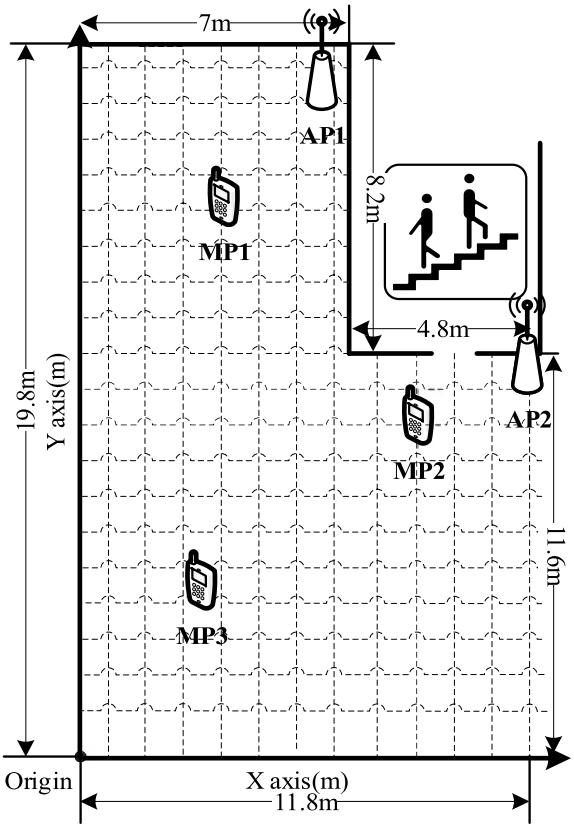

Fig. 4. Structure of experimental environment

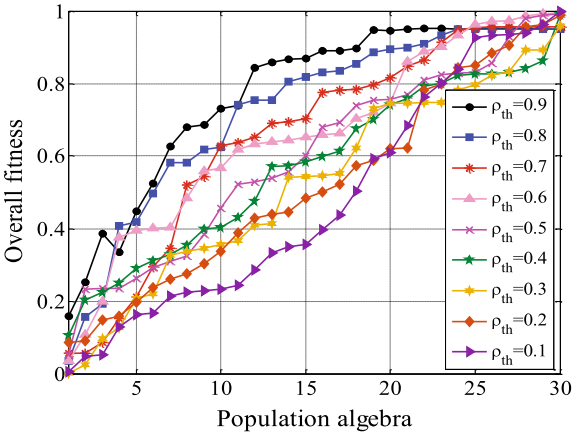

Fig. 5. Change of overall fitness

compares the average time overhead required by the 3D ray-tracing model [5], the traditional 2D ray-tracing model [6], and the proposed method for the ray modeling between each pair of AP and MP under the condition of the limited number of depth of 3. It can be seen from the table that this method performs obviously better than the methods used in the literature [5,6] in terms of time overhead.

Table 1. Average time cost for ray modeling between each pair of AP and MP

Performance index	Paper [6]	Paper [5]	The proposed
Time overhead (s)	6.03	7.25	3.41

3.3 Signal Prediction Result

Figures 6 and 7 compare the cumulative density function (CDF) of RSS prediction errors by the proposed method and the ones in [5,6] under the limited number of depth of 3, from which we can find that the proposed method performs better than the others.

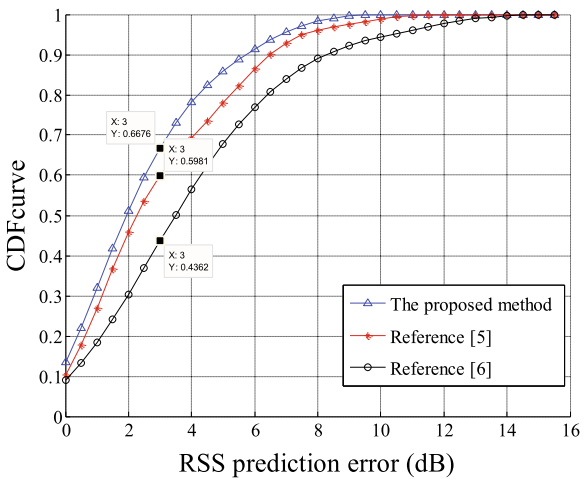

Fig. 6. CDF of errors for AP1

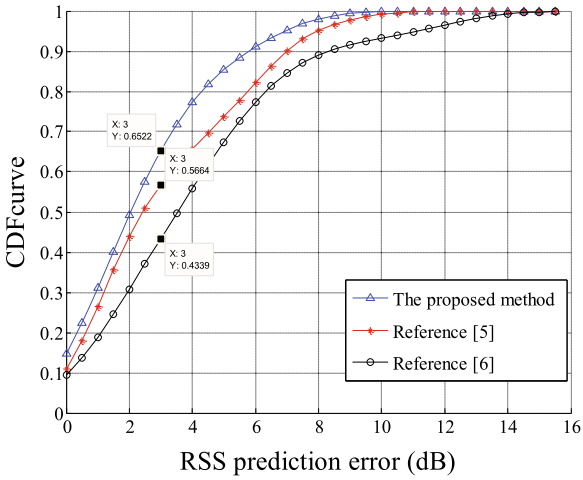

Fig. 7. CDF of errors for AP2

4 Conclusion

In this paper, we propose the adaptive-depth ray tree model, which can be used to adaptively construct a passive radio map for indoor WLAN intrusion detection. For one thing, we use the genetic algorithm to enhance the traditional quasi-3D ray-tracing model to depict the RSS variation under the indoor silence and intrusion scenarios with low labor and time cost. For another, six common signal features are allied to ensure the stability of RSS data and robustness of passive radio map. In future, we will continue to investigate a more effective passive radio map construction method to accurately locate multiple targets in the anonymous indoor WLAN environment.

Acknowledgments. This work is supported in part by the Fundamental Science and Frontier Technology Research Project of Chongqing (cstc2017jcyjAX0380).

References

1. Youssef M, Mah M, Agrawala A. Challenges: device-free passive localization for wireless environments. In: ACM international conference on mobile computing and networking; 2007. p. 222–9.
2. Jin S, Choi S. A seamless handoff with multiple radios in IEEE 802.11 WLAN. IEEE Trans Veh Technol. 2014;63(3):1408–18.
3. Wang Q, Yigitler H, Jantti R, et al. Localizing multiple objects using radio tomographic imaging technology. IEEE Trans Veh Technol. 2016;65(5):3641–56.
4. Deak G, Curran K, Condell J, et al. Detection of multi-occupancy using device-free passive localization. IET Wirel Sens Syst. 2014;4(3):130–7.
5. Liu Z, Guo L, Tao W. Full automatic preprocessing of digital map for 2.5D ray tracing propagation model in urban microcellular environment. Waves Random Complex Media. 2013;23(3):267–78.

6. Jong YLCD, Herben MAHJ. Prediction of local mean power using 2-D ray-tracing-based propagation models. IEEE Trans Veh Technol. 2001;50(1):325–31.
7. Sabar NR, Ayob M, Kendall G, et al. A dynamic multiarmed bandit-gene expression programming hyper-heuristic for combinatorial optimization problems. IEEE Trans Cybern. 2015;45(2):217–28.
8. Erceg V, Rustako AJ, Roman R. Diffraction around corners and its effects on the microcell coverage area in urban and suburban environments at 900 MHz, 2 GHz, and 6 GHz. IEEE Trans Veh Technol. 1994;43(3):762–6.
9. Dutt V, Chaudhry V, Khan I. Different approaches in pattern recognition. Comput Sci Eng. 2011;1(2):32–5.
10. Queiroz A, Trintinalia LC. An analysis of human body shadowing models for ray-tracing radio channel characterization; 2016. p. 1–5.